

Article

Nyrdvomenshor Nephrite Deposit, Polar Urals, Russia

Evgeniy V. Kislov ^{1,*}, Mikhail P. Popov ^{2,3}, Firat M. Nurmukhametov ³, Viktor F. Posokhov ¹
and Vladislav V. Vanteev ¹

¹ Dobretsov Geological Institute of the Siberian Branch of the Russian Academy of Sciences, 670047 Ulan-Ude, Russia; vitaf1@yandex.ru (V.F.P.); vanteev997@mail.ru (V.V.V.)

² Zavaritsky Institute of Geology and Geochemistry of the Ural Branch of the Russian Academy of Sciences, 620016 Ekaterinburg, Russia; popovm1@yandex.ru

³ Faculty of Geology and Geophysics, Ural State Mining University, 620014 Ekaterinburg, Russia; umuseumf@mail.ru

* Correspondence: evg-kislov@ya.ru

Abstract: We studied the quality characteristics, chemical, mineral and isotope composition of nephrite, diopsidite and rodingite of the Nyrdvomenshor nephrite deposit in the Polar Urals. We applied visual petrographic and mineralogical studies, X-ray spectral fluorescence, ICP-MS analysis, and a scanning electron microscope with a dispersive microanalysis system, to measure the oxygen isotope composition. According to its quality characteristics, the nephrite was substandard. Here, uvarovite, which forms idiomorphic grains, sometimes sheath-like and less often xenomorphic elongated, and substituting the chromite, was commonly encountered. The nephrite was formed due to both metamorphic and metasomatic processes. The serpentinite was replaced by diopsidite, which was then replaced by nephrite. The metamorphism intensified the metasomatism of the serpentinite melange and provided the cryptocrystalline tangled-fibrous structure of the nephrite. Then, metamorphism and metasomatism led to the formation of omphacite and the cracking of the nephrite, which reduced its quality. As these processes progressed, the contribution of the crustal fluid increased.

Keywords: nephrite; diopsidite; rodingite; Nyrdvomenshor; Polar Urals; uvarovite; chromite; metamorphism; metasomatism



Citation: Kislov, E.V.; Popov, M.P.; Nurmukhametov, F.M.; Posokhov, V.F.; Vanteev, V.V. Nyrdvomenshor Nephrite Deposit, Polar Urals, Russia. *Minerals* **2023**, *13*, 767. <https://doi.org/10.3390/min13060767>

Academic Editors: Guanghai Shi, Tao Chen and Liang Zhang

Received: 16 April 2023

Revised: 23 May 2023

Accepted: 31 May 2023

Published: 2 June 2023



Copyright: © 2023 by the authors. Licensee MDPI, Basel, Switzerland. This article is an open access article distributed under the terms and conditions of the Creative Commons Attribution (CC BY) license (<https://creativecommons.org/licenses/by/4.0/>).

1. Introduction

Nephrite consist of fibrous tremolite or actinolite. The general formula for the tremolite-actinolite-ferroactinolite isomorphous series is $\text{Ca}_2(\text{Mg,Fe})_5\text{Si}_8\text{O}_{22}(\text{OH})_2$. It is a highly valuable jewelry and ornamental stone, long used by humankind, and especially popular in China and New Zealand. The most expensive samples are white translucent, black and bright green with a minimum amount of ore minerals, or with the “cat’s eye” effect nephrites, as well as alluvial pebbles with edges of coloring.

Nephrite deposits belong to two endogenous geological industrial types: those formed at the ultramafic metasomatites of ophiolites (serpentinite type, S-type) and those formed at the carbonate tremolite-calcite magnesian skarns (dolomite type, D-type) [1,2]. Deposits of the S-type are a source of predominantly green, brown and black nephrite, while deposits of the D-type produce mainly light-colored nephrite, in colors from white through to light green and brown (honey), due to the fact that the oxidation of divalent iron to trivalent, black nephrite, is less common [3,4]. The Dahua deposit in the Guangxi Zhuang Autonomous Region [3] and the Luodian deposit in Guizhou Province [5] in southern China, formed on the contact of diabases and limestones, are close to the D-type. The exogenous geological industrial type is represented by placers, of which the alluvial ones are the most productive.

In China, D-type nephrite deposits are the most common, so they are the best studied. There are few deposits of S-type nephrite outside of Russia. In China, the Manas deposit

in the Northern Tien Shan in the Xinjiang Uygur Autonomous Region is practically exhausted [6,7]. Nephrite of both the S-type and D-type is mined from the famous Golmud deposit in the central part of Qinghai Province [8]. The Yushigou (Qilian) S-type nephrite deposit is mined in the north of Qinghai Province [9]. The Shimian deposit in Sichuan Province is famous for producing high-quality nephrite with chatoyancy [10,11]. The Fengtien S-type nephrite deposit is known in Taiwan [12–14]. Recently, nephrite from the border areas of Pakistan and Afghanistan has appeared on the market [15–18]. The Dzhetysay nephrite occurrence is on the southern extension of the Urals in Kazakhstan [19]. The Shaitantas deposit in the Karaganda region of Kazakhstan [20], and the Co Phuong deposit in Shonla Province in Vietnam [21] have been poorly studied.

A number of S-type nephrite deposits are located on the Pacific coast, and mining is carried out mainly in British Columbia in Canada [22–25]. Nephrite deposits are known, but poorly studied, in Wyoming [26] and several other states of the USA. The Jordanov and Naslawice deposits in Poland were mainly exhausted in the XIX century, when they were located in the territory of Prussia under the names Jordansmühl and Naselwitz [26–28]. A few nephrite occurrences are known in Switzerland, Italy and Austria. Small S-type nephrite deposits have long been known on the South Island of New Zealand [26,29–31] and in New South Wales in Australia [32,33].

As of 1 January 2022, the Russian State Reserve balance includes 26 nephrite deposits. Seven deposits are being developed in the Buryatia Republic, including the S-type nephrite deposits: Khamarkhuda in the Khamar-Daban and Ospa (22.99% of Russian reserves and 47.64% of Russian production) in the Eastern Sayans. Deposits of the S nephrite type Kurtushiba (Eastern Section) in the Western Sayans, in the Tuva Republic, and also Onot in the Eastern Sayans, in the Irkutsk region, Arakhushanzhalga, the Pole Tchudes (Field of Miracles), Ulan-Khoda, Khusha-Gol, and Gorlykgol (with 25.15 and 6.95%, respectively) in the Eastern Sayans, Buryatia, have been prepared for development. The deposits of Kantegir and Kurtushiba (Central Section), Stan-Taskyl in the Western Sayans, the Krasnoyarsk region and Sagan-Sayr in the Eastern Sayans, Buryatia are being explored. The unallocated mineral resources fund (not transferred to development) includes the Academia deposit in the Southern Urals, Chelyabinsk region, Boldokit and Zun-Ospa in the Eastern Sayans, and Khangarul and Kharganta in the Khamar-Daban, Buryatia. Many occurrences that have not been put on the State Balance sheet are also being explored.

A number of small deposits of S-type nephrite are known in the Urals. The first single finds were made in the area of Muldakaev [34,35] and on Mount Bikilar [34,35] in the area of Miass in the Southern Urals. The Nyrdvomenshor deposit is known in the Polar Urals [20,36]. In the Middle Urals, nephrite was found in the alluvium of Neivo-Rudyanka, near the town of Pyshma [37] and the Bazhenov chrysotile asbestos deposit [35].

There are three nephrite occurrences in the Bashkir Republic: Kozma-Demyan, near the talc deposit of the same name in the north-east of Bashkiria—nephrite blocks on the banks of the Maly Iremel River; in the south-east of Bashkiria, Keusht—primary outlets with an area of 1.5–2 m²; and Kildigul, on the right side of the valley of the Saraga River—a primary outlet, 10 × 5 m in size, in the polymict serpentinite melange of the Kraka complex [38]. The Khalil nephrite deposit was discovered in 1968 in the Khalil ultramafic massif in the Orenburg region [20].

In 2003, the Akademia deposit with the Student and Faculty sites was discovered in the vicinity of Miass in the Chelyabinsk region [39]. There is the Uchaly-Miass potentially nephrite-bearing area traced from north to south from the city of Karabash through Miass to the city of Uchaly [34]. Nevertheless, in the Urals, nephrite was mined in a limited volume at the Nyrdvomenshor and Academia deposits. At present, mining is not performed here.

Despite the significant number of deposits and occurrences of S-type nephrite, its geology and genesis has not been sufficiently studied. The idea of a metasomatic origin of the nephrite is the most popular [1,2], and some authors hold an opinion about the predominant role of metamorphism [40]. This study is aimed at studying the material composition of the nephrite at the Nyrdvomenshor deposit in order to clarify the features

of its origin. Previously, part of the material of this article was published in abstracts in Russian [41].

2. Materials and Methods

In order to assess the quality and composition of the nephrite from the Nyrdvomenshor deposit, which includes the Nyrdvomenshor and Ray-Iz sites, we studied 8 polished plates of alluvial material. An angular rodingite sample and a polished jadeite plate were examined as additional material.

Visual petrographic and mineralogical studies were performed in natural light, using photofixation. Decorative properties (color, shade, pattern, presence of edges, degree of roughness) were determined using an MBS-10 binocular microscope and a special CYZ-B05 flashlight.

The chemical composition of the rocks was determined using the X-ray spectral fluorescence method on an XRF-1800 wave X-ray fluorescence spectrometer (Shimadzu, Kyoto, Japan) at the “Geoanalytic” Research Center at IGG UrB RAS, Ekaterinburg, according to the method in [42], and the analysts N.P. Gorbunova, L.A. Tatarinova, I.A. Zhelunitsyn and A.A. Nekrasova.

The samples were decomposed and the impurity element content was analyzed using ICP-MS analysis at the “Geoanalytic” Research Center at IGG UrB RAS, by analyst D.V. Kiseleva, on a NexION300S quadrupole ICP mass spectrometer, Perkin Elmer, USA. The microwave decomposition of the samples was carried out using a mixture of HCl + HNO₃ + HF acids, using the Berghof Speedwave MWS 3+ system. Typical operating conditions of the mass spectrometer are as follows: the power of the radio frequency generator is 1300 W and the material of the interface cones is platinum. All measurements were carried out in the mode of quantitative analysis, with the construction of calibration curves. Multi-element standard solutions certified in accordance with ISO 9001 Perkin Elmer Instruments were used to construct the calibration dependencies. Certified samples of BCR-2 basalt and AGV-2 andesite USGS were used to control the correctness and accuracy while determining the trace element composition. The obtained concentrations of scattered, rare-earth and trace elements correspond to the certified values, with an acceptable deviation of within 15%. The errors in element identification are (rel. %): 24 (Cr, Ni, Co, Cu, V, Ba, Sr), 30 (Rb), 41 (REE), 50 (Zr), and 60 (Y, Hf, Ta, Nb, Th, U).

The mineral composition was studied using a LEO-1430VP scanning electron microscope, Carl Zeiss, Germany, with the INCA Energy 350 energy dispersive microanalysis system, Oxford Instruments, UK, at the “Geospectr” Research Center at GIN SB RAS, Ulan-Ude, by the analyst E.A. Khromova. The research conditions are as follows: accelerating voltage—20 kV, probe current—0.3–0.4 nA, probe size—<0.1 microns, and measurement time—50 s (live time), with the analysis error in the amount reaching 2–4 wt. %, depending on the quality of the sample surface and the characteristics of its composition. The content of trivalent iron was calculated using stoichiometry.

The oxygen isotope composition was measured on a FINNIGAN MAT 253 gas mass spectrometer at the “Geospectr” Research Center at GIN SB RAS, Ulan-Ude, by the analyst V.F. Posokhov, using the double intake system in the classical version, with a standard sample. To determine $\delta^{18}\text{O}$ values, the samples were prepared using the laser fluorination (LF) method in the mode “laser ablation with oxygen extraction from silicates” in the presence of a BrF₅ reagent, according to the method in [43]. The calculations were carried out with respect to the O₂ working standard, and calibrated using the V-SMOW scale by regular oxygen measurements for the international standards for NBS-28 quartz and NBS-30 biotite. The correctness of the values obtained was controlled by regular measurements of the center’s own internal standard for GI-1 quartz and laboratory IGEM RAS Polar quartz. The measurement error of the obtained $\delta^{18}\text{O}$ values was at the level of (1 s) \pm 0.2%.

3. Results

3.1. Geology of Nyrdvomenshor Deposit

The Nyrdvomenshor deposit is located on the contact of the Rai-Iz ultramafite massif in the Polar Urals with metamorphic and intrusive rocks at the basin of the upper and middle reaches of the Nyrdvomenshor stream, 56 km northwest of Labytnangi town in the Priuralsky district of the Yamalo-Nenets Autonomous Okrug.

Nephrite was found here in 1974 by the “Sevkvartssamotsvety” enterprise. In 1975–1980, 250 nephrite and 60 jadeite locations were found in the bedrock and boulder placers. Some of them were industrially assessed and underwent pilot testing with inventory calculation. In 1980–1981, 21.8 tons of ornamental nephrite (1st grade) were mined from alluvial placers. Protocol No. 20\7 of 26 February 1982 from the Ministry of Geology of the USSR approved the nephrite reserves of 21.8 tons. In 1985–1990, the Polar-Ural Geological Exploration Expedition performed a 1:50,000 survey of this area. In 1991, the “Nord Rifei” enterprise reassessed the nephrite and jadeite sites. Protocol No. 46\91 of 28 December 1991 from the “Zapsibkomgeologiya” geological section tested the forecast resources: nephrite—1000 tons; jadeite—5000 tons, jasper—10,000 tons.

On the 14 October 2013, the Department for Subsoil Use in the Yamalo-Nenets Autonomous Okrug put up the Nyrdvomenshor site (nephrite, jadeite, jasper) for auction. Four companies submitted an application, but were not admitted to the auction, and the auction did not happen. On the 31 July 2014, the authorities of the Yamalo-Nenets Autonomous Okrug established the Polar-Urals Nature Park, which included the territory of the licensed area. According to protocols No. 24-TV of 25 December 2019 and No. 12-TV of 6 October 2020, “NTS-Uralnedra” tested the forecasted resources of nephrite, jadeite and jasper of the Rai-Iz site, which was not included in the natural park, and found the following: nephrite (raw)—3000 tons; jadeite (raw)—15,000 tons; jasper (raw)—11,000 tons. On the 9 November 2020, the Department for Mineral Resources in the Ural Federal District announced an auction for the right to use the subsoil for the purpose of the geological study, exploration and extraction of nephrite, jadeite and jasper at the Rai-Iz site. According to the results of the auction, the license was issued to the “Salekhard Mining Enterprise”.

The deposit is confined to the zone of northern tectonic contact along the Main Ural fault of the Rai-Iz ultramafic massif with metamorphic and intrusive rocks of the Harbey block of the Middle-Late Proterozoic and metamorphosed sedimentary-volcanogenic rocks of the Lemvin structural-facies zone of the Paleozoic age (Figure 1). The Rai-Iz massif is composed mainly of harzburgites, dunites and serpentinites, formed after these [20,44]. Paleozoic sedimentary-volcanogenic formations are represented by clay-siliceous and carbonaceous-siliceous shales with interlayers of metaeffusives of ultramafic composition. The contact of the Rai-Iz massif along the Main Ural fault is a zone of polymictic melange with formations of diopsidites, rodingites, plagioclasites, albite-jadeitites, and nephrites. Eluvial-deluvial, fluvioglacial and alluvial deposits are common.

Nephrite sites are known to be in bedrocks, piles and placers, mostly in the area of the Nyrdvomenshor and Kharamatalaus faults (Figure 2) within serpentine melange (Figure 3), in the contact zones of after-gabbro bodies. In the bedrock, nephrite forms with more than 300 lenticular veins, with a length of 1–60 m and a thickness of several centimeters to 3 m. There are five main types of nephrite localization: the veins in serpentinites; in the contact zone of serpentinites and metaeffusives; metaeffusives; in the contact zone of after-gabbroid rodingites and serpentinites; and in rodingites [20].

The erosion of most nephrite veins provided the bulk of block-boulder material that makes up the industrial glacial-alluvial placer deposit—the main object of nephrite extraction (Figure 4). During the boulder transportation, there was a natural improvement in the quality of nephrite, due to abrasion of the talc-tremolite sheath [20]. The alluvial placer of nephrite is confined to the channel and floodplain parts of the Nyrdvomenshor Creek and its tributaries—the Nephritovyi and Obraztsovyyi streams. The width of the placer ranges from 20 to 60 m, and the length is up to 4.5 km. The size of the nephrite boulders is 0.1–2.9 m. The average frequency of occurrence is 1 boulder per 680–700 m².

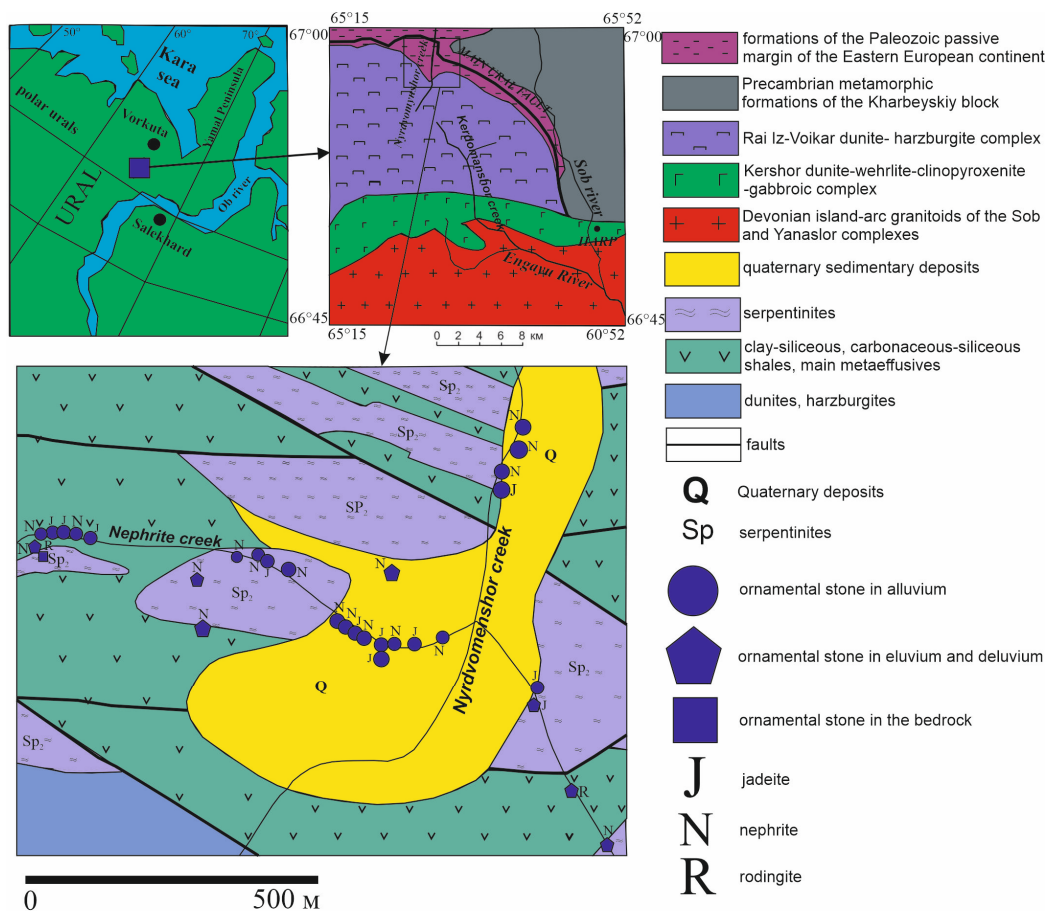


Figure 1. Scheme of the Nyrdvomenshor deposit. The right inset shows the eastern part of the Rai-Iz massif, according to [45].

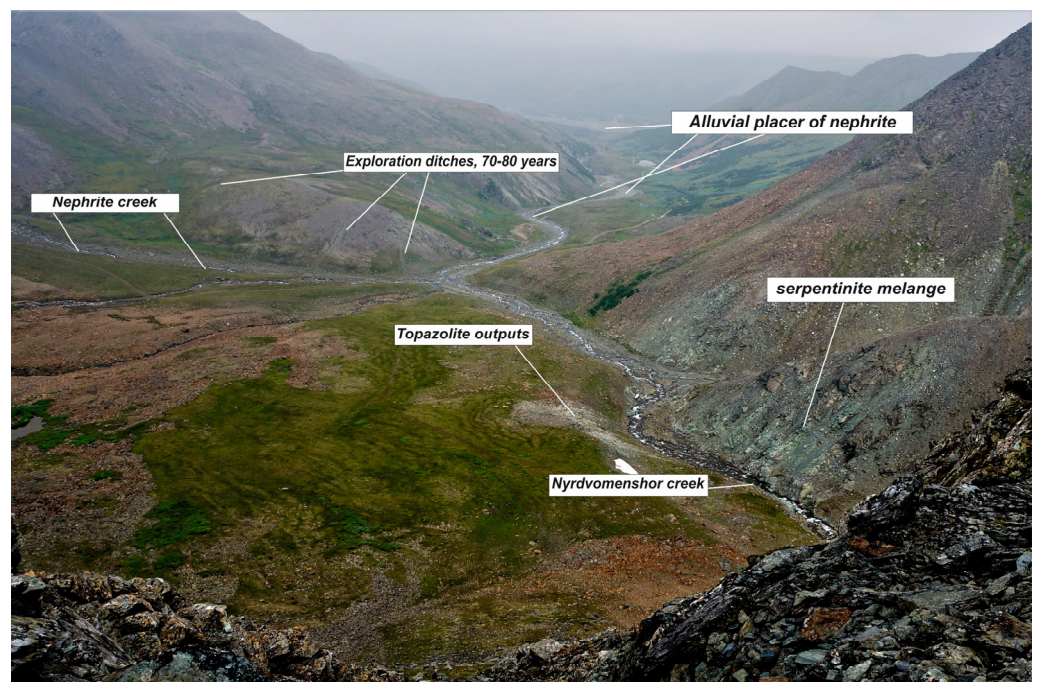


Figure 2. Photo of the Nyrdvomenshor deposit.



Figure 3. Block of nephrite in serpentine melange.



Figure 4. Alluvial block of nephrite.

3.2. Diopside and Rodingite

The two samples, 162 and 3/12 (Figure 5), are represented by diopsidites, “karkaro” [1]. No. 162 is grayish-white with greenish streaks of uvarovite and black grains of chromite, while no. 3/21 is of a heterogeneous light-green color, due to the uneven distribution of tremolite and chlorite.

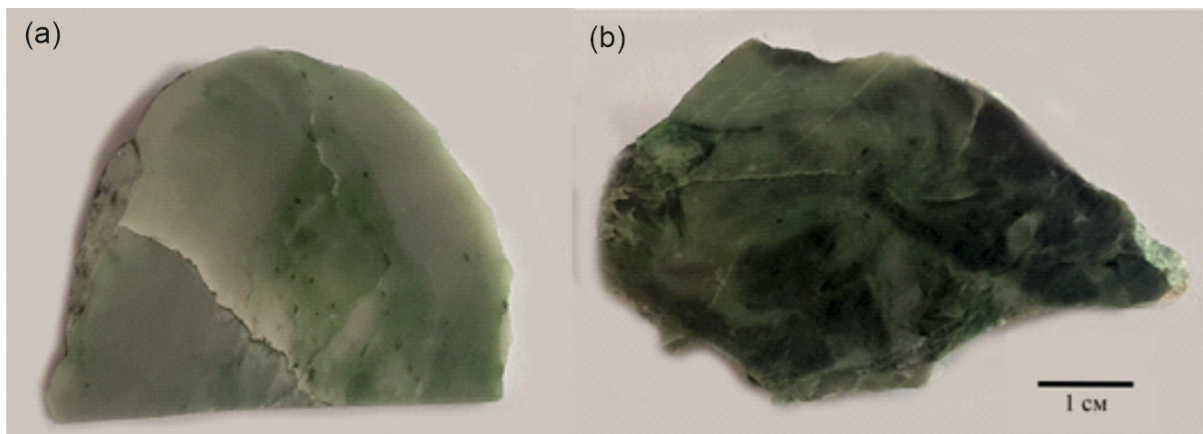


Figure 5. Diopside samples: (a)—162; (b)—3/21.

Fine-grained diopside $(\text{Ca}_{0.94}\text{Fe}_{0.02}\text{Mn}_{0.01}\text{Al}_{0.02}\text{Si}_{0.01})_{\Sigma 1}(\text{Mg}_{0.87}\text{Fe}_{0.13})_{\Sigma 1}\text{Si}_{2.00}\text{O}_6$ (Table 1) prevails in the composition of diopside; cloud-like aggregates of chlorite $(\text{Mg}_{4.43}\text{Fe}^{2+}_{0.57})_{\Sigma 5}\text{Al}_{1.00}(\text{Si}_{3.36}\text{Al}_{0.37}\text{Cr}_{0.10}\text{Fe}^{3+}_{0.03}\text{Ca}_{0.03})_{\Sigma 3.89}\text{O}_{10}(\text{OH})_8$, streaks of chlorite with grains of chromite $(\text{Fe}^{2+}_{0.62}\text{Mg}_{0.35}\text{Mn}_{0.02}\text{Zn}_{0.02})_{\Sigma 1.01}(\text{Cr}_{1.19}\text{Al}_{0.75}\text{Fe}^{3+}_{0.17}\text{Ti}_{0.01})_{\Sigma 2.12}\text{O}_4$ and uvarovite $(\text{Ca}_{2.84}\text{Mg}_{0.11}\text{Fe}^{2+}_{0.09}\text{Mn}_{0.01})_{\Sigma 3.05}(\text{Cr}_{1.15}\text{Al}_{0.70}\text{Fe}^{3+}_{0.11}\text{Ti}_{0.04})_{\Sigma 2}(\text{Si}_{2.92}\text{Ti}_{0.08})_{\Sigma 3}\text{O}_{12}$ (one analysis corresponds to andradite $(\text{Ca}_{2.96}\text{Mg}_{0.05})_{\Sigma 3.01}(\text{Fe}^{3+}_{1.42}\text{Cr}_{0.42}\text{Ti}_{0.08})_{\Sigma 1.92}\text{Si}_{3.07}\text{O}_{12}$), small idiomorphic and xenomorphic grains of heazlewoodite $\text{Ni}_{2.95}\text{Fe}_{0.01}\text{S}_{2.04}$ (in 6 grains of sample 162, Ni—71.46%–74.23%, S—25.75%–27.72%, in 3 grains of sample 3/31, Fe—0.67%–2.22%, Ni—62.90%–71.77%, S—26.20%–33.25%) are characteristic. Chromite grains are split by chlorite veins. Uvarovite corrodes and overgrows the chromite. Tremolite $(\text{Ca}_{1.83}\text{Al}_{0.11}\text{Fe}_{0.03}\text{Na}_{0.03})_{\Sigma 2}(\text{Mg}_{4.53}\text{Fe}_{0.50})_{\Sigma 5.03}\text{Si}_{7.97}\text{O}_{22}(\text{OH})_2$, pentlandite with an admixture of cobalt $\text{Fe}_{3.59}\text{Co}_{0.10}\text{Ni}_{5.45}\text{S}_{7.77}$, stibnite with an admixture of iron intergrown with heazlewoodite, titanite $(\text{Ca}_{0.97}\text{Fe}_{0.02})_{\Sigma 0.98}(\text{Ti}_{0.96}\text{Al}_{0.03})_{\Sigma 0.99}\text{Si}_{1.04}\text{O}_5$ with an inclusion of ilmenite $(\text{Fe}_{0.90}\text{Mn}_{0.08})_{\Sigma 0.98}\text{Ti}_{1.01}\text{O}_3$, in a small amount, appear in sample 3/21, and the tremolite makes cracks in the chromite.

Local light-green rodingite with a yellowish shade is traditionally called “californite”, that is, Californian jade. However, as a result of the sample analysis, it turned out that it consists of hydrogrossular $\text{Ca}_{2.89}\text{Al}_{2.00}\text{Si}_{2.89}\text{O}_{12}(\text{OH})_{0.11}$ (Table 2), that is, it should be attributed to Transvaal jade. There are minor amounts of vesuvianite $\text{Ca}_{9.30}(\text{Mg}_{0.85}\text{Fe}_{0.60}\text{Al}_{0.30})_{\Sigma 1.75}\text{Al}_{4.00}(\text{Si}_{1.00}\text{O}_4)_5(\text{Si}_{1.80}\text{Al}_{0.20}\text{O}_7)_2(\text{OH})_4$ and chlorite $(\text{Mg}_{3.82}\text{Fe}^{2+}_{0.82}\text{Al}_{0.32})_{\Sigma 4.96}\text{Al}_{1.00}(\text{Si}_{2.80}\text{Al}_{1.20})_{\Sigma 4}\text{O}_{10}(\text{OH})_8$, forming veinlets and cloud-like aggregates.

The chemical analysis of another sample (Table 3) indicates that Californian jade, that is, vesuvianite, is also present at the deposit.

Table 1. Chemical composition of minerals in diopsidites, wt. %.

	Diopside		Garnet		Tremolite		Chlorite		Titanite		Chromite		Ilmenite
	Mean <i>n</i> = 14	Range	Mean <i>n</i> = 11	Range	Mean <i>n</i> = 4	Range	Mean <i>n</i> = 3	Range			Mean <i>n</i> = 7	Range	
SiO ₂	55.01	52.86–57.44	36.15	35.62–37.91	57.37	55.49–58.85	33.51	32.86–34.38	32.08	32.41	0	0	0
TiO ₂	0.02	0–0.35	1.94	0.90–3.12	0.03	0–0.38	0	0	38.60	39.45	0.06	0–0.42	51.28
Al ₂ O ₃	0.44	0–1.70	6.88	0–10.68	1.09	0–3.95	12.29	6.97–15.17	0.74	0.59	20.38	12.17–28.40	0
Cr ₂ O ₃	0.16	0–0.63	14.75	6.23–19.83	0	0	2.12	0.64–4.90	0	0	45.09	39.07–58.75	0
FeO	4.20	2.38–12.43	1.64	0.90–4.35	4.24	4.05–4.43	7.63	6.64–9.16	0	0.58	19.74	12.49–29.56	43.30
Fe ₂ O ₃	0.01	0–0.10	3.45	0–20.27	-	-	-	-	-	-	3.61	1.40–7.09	-
MnO	0.12	0–0.58	0.18	0–0.58	0.14	0–0.56	0	0	0	0	0.38	0–1.08	3.67
MgO	15.94	11.67–17.96	0.81	0–3.42	19.26	11.92–22.07	29.66	28.31–31.77	27.49	27.76	9.49	2.28–15.55	0
CaO	23.80	20.85–24.95	32.41	29.58–34.08	14.12	12.41–18.19	0.61	0.27–0.99	0	0	0	0	0
Na ₂ O	0.19	0–1.04	0	0	1.11	0–3.79	0	0	0	0	0	0	0
NiO	0	0	0	0	0	0	0	0	0	0	0.94	0–3.21	0
ZnO	0	0	0	0	0	0	0	0	0	0	0.05	0–0.34	0
V ₂ O ₃	0	0	0	0	0	0	0	0	0	0	0.04	0–0.32	0
Total	99.89		98.21		97.36		85.82		98.91	100.79	99.78		98.24

Notes: *n*—the number of analyses.

Table 2. Chemical composition of minerals in rodingite, wt. %.

	Hydrogrossular		Chlorite		Vesuvianite	
	Mean <i>n</i> = 5	Range	Mean <i>n</i> = 5	Range	Mean <i>n</i> = 4	Range
SiO ₂	36.36	34.00–37.40	27.78	24.62–31.13	35.09	34.06–36.24
Al ₂ O ₃	21.34	19.78–22.20	21.15	18.31–25.32	16.35	16.16–16.67
FeO	0.30	0–0.74	9.58	2.97–16.52	2.86	2.80–3.04
MgO	0	0	25.49	21.23–31.54	2.38	2.16–2.65
CaO	37.24	36.17–38.13	0	0	35.57	34.24–36.28
Total	95.24		84.00		92.25	

Notes: *n*—the number of analyzes.**Table 3.** Chemical composition of the rocks of the Nyrdvomenshor deposit, main components by wt. %, trace elements in ppm.

	Nephrite		Diopsidite		Rodingite
SiO ₂	58.17	58.44	56.35	52.83	33.70
TiO ₂	0.03	0.03	0.04	0.08	0.05
Al ₂ O ₃	0.33	0.28	0.66	0.40	19.48
Fe ₂ O ₃ Γ	5.07	4.87	5.88	8.13	5.19
MnO	0.10	0.11	0.11	0.11	0.04
MgO	21.70	21.68	21.49	16.42	10.91
CaO	12.57	12.06	13.04	21.40	28.80
Na ₂ O	0.15	0.48	0.27	0.08	0.07
K ₂ O	0.06	0.19	0.11	0.04	0.03
P ₂ O ₅	0	0.02	0.03	0.09	0
S	0.03	0.03	0.03	0.04	0
Cr	0.02	0.03	0.08	0.01	0.01
LOI	1.87	2.03	2.36	0.57	1.78
Σ	100.09	100.26	100.42	100.20	100.08
Li	0.5	0.5	1.5	1	14
Be	0.11	0.2	0.23	0.25	0.013
Sc	2.8	3.7	6	5	12
Ti	40	40	60	210	110
V	15	15	16	21	26
Cr	400	440	700	380	70
Mn	340	400	380	380	170
Co	21	24	24	18	14
Ni	400	400	400	200	60
Cu	4	4	9	11.5	4
Zn	14	15	20	9	6
Ga	0.4	0.4	0.8	0.5	3
Ge	0.44	0.39	0.27	0.6	0.34
As	<0.02	<0.02	<0.02	<0.02	<0.02
Se	0.17	0.2	0.24	0.35	0.45
Rb	0.5	0.21	0.19	0.27	0.33
Sr	33	29	50	40	27
Y	0.17	0.3	0.6	2	0.8
Zr	0.19	0.16	0.4	6	0.8
Nb	0.26	0.19	0.16	0.4	0.08
Mo	0.29	0.28	0.28	0.6	0.29
Ag	0.0117	0.0111	0.0072	0.019	0.008
Cd	0.025	0.03	0.07	0.03	0.04
Sn	0.24	0.16	0.2	0.32	0.21
Sb	0.07	0.07	0.08	0.4	0.09
Te	<0.01	0.019	<0.01	0.017	<0.01
Cs	0.04	0.012	0.027	0.02	0.08
Ba	5.4	4.8	4.9	5.1	4.7
La	0.05	0.07	0.13	1.2	0.09
Ce	0.14	0.16	0.24	2.3	0.18
Pr	0.019	0.024	0.033	0.31	0.027
Nd	0.078	0.11	0.16	1.2	0.13
Sm	0.022	0.036	0.044	0.3	0.049
Eu	0.043	0.02	0.019	0.09	0.049
Gd	0.027	0.046	0.063	0.38	0.087
Tb	0.005	0.007	0.013	0.06	0.019
Dy	0.028	0.038	0.08	0.38	0.15
Ho	0.006	0.007	0.018	0.08	0.035
Er	0.017	0.021	0.059	0.24	0.11
Tm	0.0028	0.0031	0.009	0.035	0.016
Yb	0.019	0.026	0.07	0.22	0.12
Lu	0.003	0.005	0.01	0.04	0.019
Hf	0.1	0.024	0.023	0.21	0.04
Ta	0.13	0.05	0.037	0.11	0.045
W	0.3	0.26	0.4	0.8	3
Tl	0.004	0.003	0.005	0.0025	0.0027
Pb	0.19	0.3	0.6	0.8	0.6
Bi	0.0142	0.0051	0.0033	0.019	0.0039
Th	0.08	0.018	0.011	0.3	0.018
U	0.014	0.013	0.031	0.16	0.011

3.3. Characteristics of Nephrite

Nephrite is mostly heterogeneously colored; a homogeneous color is less common (Figure 6). It is a trickle-like grayish-green to olive-green; dark grayish-green, often with spots, with flakes of a lighter grayish-green color up to 3 mm across. Thin, rare grains of ore minerals are characteristic. Ore mineral grains of up to 2 mm in size, making up to 3% of the sample area, are evenly distributed. In sample 2/21, there are numerous visually distinguishable needle-like tremolite crystals all over the surface. One can see matte weathering crusts of a lighter grayish-green color up to 0.5 cm thick. The translucency is up to 0.2 cm.

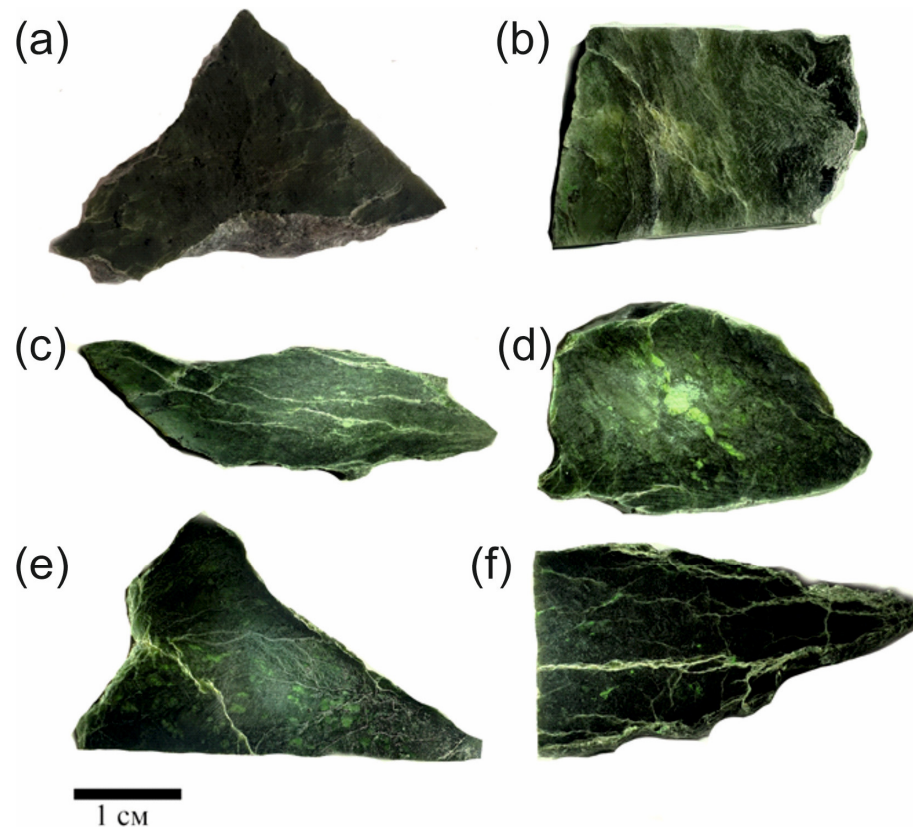


Figure 6. Nephrite samples: (a)—558; (b)—61-2; (c)—2/21; (d)—1/21; (e)—510-1; (f)—557-1.

Intense fracturing is observed, and in sample 2/21 it reaches foliation. Nephrite reacts badly to polishing, with intense shagreen and notches. Mirror polishing occurs less often, but with cracks, or shagreen, there is an undulated pattern and cracks. Polishing is often heterogeneous: areas of extraneous mineral formation in practice do not respond to a polish, and they remain matte.

3.4. Mineral Composition of Nephrite

We studied the mineral composition of the nephrite. It is dominated by cryptocrystalline tremolite ($\text{Ca}_{1.90}\text{Na}_{0.04}\text{K}_{0.02}\text{Al}_{0.02}\text{Si}_{4.99}\text{O}_{22}(\text{OH})_2$) ($\Sigma 1.98$) ($\text{Mg}_{4.53}\text{Fe}_{0.45}\text{Mn}_{0.01}\text{Si}_{8.02}\text{O}_{22}(\text{OH})_2$) (Table 4) diverse in morphology from fine-fibrous (Figure 7a,b) to rare radiaxial (Figure 7c). There are also larger, individual needle-like crystals (Figure 7g,h). The diopside ($\text{Ca}_{0.87}\text{Na}_{0.05}\text{Fe}^{3+}_{0.02}\text{Mn}_{0.01}\text{Si}_{2.01}\text{O}_6$) ($\Sigma 0.95$) ($\text{Mg}_{0.91}\text{Fe}^{2+}_{0.08}\text{Al}_{0.02}\text{Cr}_{0.02}\text{Si}_{2.01}\text{O}_6$) (Table 4) forms relict grains (Figure 7e). The omphacite ($\text{Ca}_{0.62}\text{Na}_{0.35}\text{Fe}^{3+}_{0.03}\text{Mn}_{0.02}\text{Si}_{2.00}\text{O}_6$) ($\Sigma 1.02$) ($\text{Mg}_{0.54}\text{Cr}_{0.20}\text{Al}_{0.19}\text{Fe}^{2+}_{0.10}\text{Si}_{2.00}\text{O}_6$) (Table 4, Figure 7a) overgrows the grains of the chromite ($\text{Mg}_{0.48}\text{Fe}^{2+}_{0.46}\text{Mn}_{0.02}\text{Zn}_{0.01}\text{Cr}_{1.17}\text{Al}_{0.61}\text{Fe}^{3+}_{0.20}\text{Ti}_{0.01}\text{O}_4$) ($\Sigma 1.98$) and uvarovite ($\text{Ca}_{2.84}\text{Fe}^{2+}_{0.09}\text{Mg}_{0.07}\text{Cr}_{1.18}\text{Al}_{0.38}\text{Fe}^{3+}_{0.29}\text{Ti}_{0.05}\text{Mn}_{0.04}\text{V}_{0.01}\text{Si}_{1.00}\text{O}_4$) ($\Sigma 3.00$) (Table 4).

Table 4. Chemical composition of nephrite minerals, wt. %.

	Tremolite		Uvarovite		Diopside		Omphacite		Chlorite		Shuiskite Group Mineral		Chromite	
	Mean <i>n</i> = 35	Range	Mean <i>n</i> = 24	Range	Mean <i>n</i> = 7	Range	Mean <i>n</i> = 10	Range	Mean <i>n</i> = 5	Range	Mean <i>n</i> = 6	Range	Mean <i>n</i> = 23	Range
SiO ₂	58.15	56.65–59.99	34.75	33.93–37.87	54.83	53.98–55.24	54.77	52.28–56.31	33.56	31.75–35.26	21.01	11.96–27.36	0	0
TiO ₂	0.01	0–0.35	0.85	0–2.53	0.04	0–0.30	0	0	0	0	0.33	0–1.53	0.33	0–1.83
Al ₂ O ₃	0.10	0–0.66	3.91	0.43–9.31	0.11	0–2.42	4.45	0.76–6.59	10.84	9.07–12.34	3.64	1.59–6.76	18.86	0–38.60
Cr ₂ O ₃	0	0	18.25	12.32–22.01	0.84	0–1.77	4.86	2.59–10.11	4.06	2.40–5.89	29.04	24.44–33.10	46.62	40.38–58.54
FeO	3.92	2.98–4.80	1.39	0–3.33	2.48	0.98–3.49	3.34	0.61–6.03	7.51	6.73–8.17	23.70	13.05–39.30	16.31	11.24–27.92
Fe ₂ O ₃	-	-	5.45	0.47–14.48	0.73	0–2.13	1.29	0–4.04	-	-	-	-	5.40	1.38–22.95
MnO	0.04	0–0.37	0.56	0–1.28	0.31	0–0.50	0.51	0–2.47	0	0	1.78	0.99–2.43	0.54	0–3.49
MgO	22.09	20.18–23.45	0.74	0–2.72	16.09	14.33–17.44	9.90	5.99–12.04	30.09	29.12–30.74	0.14	0–0.86	11.66	0.66–17.68
CaO	12.69	11.75–13.75	32.39	30.80–34.73	23.79	21.97–24.91	15.76	12.20–18.23	0.14	0–0.71	18.97	11.05–24.95	0	0
Na ₂ O	0.19	0–0.85	0	0	0.83	0–1.95	4.96	3.38–6.31	0.13	0–0.65	0.08	0–0.49	0	0
K ₂ O	0.11	0–0.51	0	0	0	0	0	0	0	0	0	0	0	0
CoO	0	0	0	0	0	0	0	0	0	0	0	0	0.05	0–0.64
NiO	0	0	0	0	0	0	0	0	0	0	0	0	0.02	0–0.43
ZnO	0	0	0	0	0	0	0	0	0	0	0.78	0–1.57	0.13	0–1.79
V ₂ O ₃	0	0	0.17	0–1.26	0	0	0	0	0	0	0	0	0.03	0–0.43
Cl	0.02	0–0.40	0	0	0	0	0	0	0	0	0	0	0	0
F	0.04	0–1.48	0	0	0	0	0	0	0	0	0	0	0	0
Total	97.36		98.46		100.05		99.84		86.33		99.47		98.24	

Notes: *n*—the number of analyses.

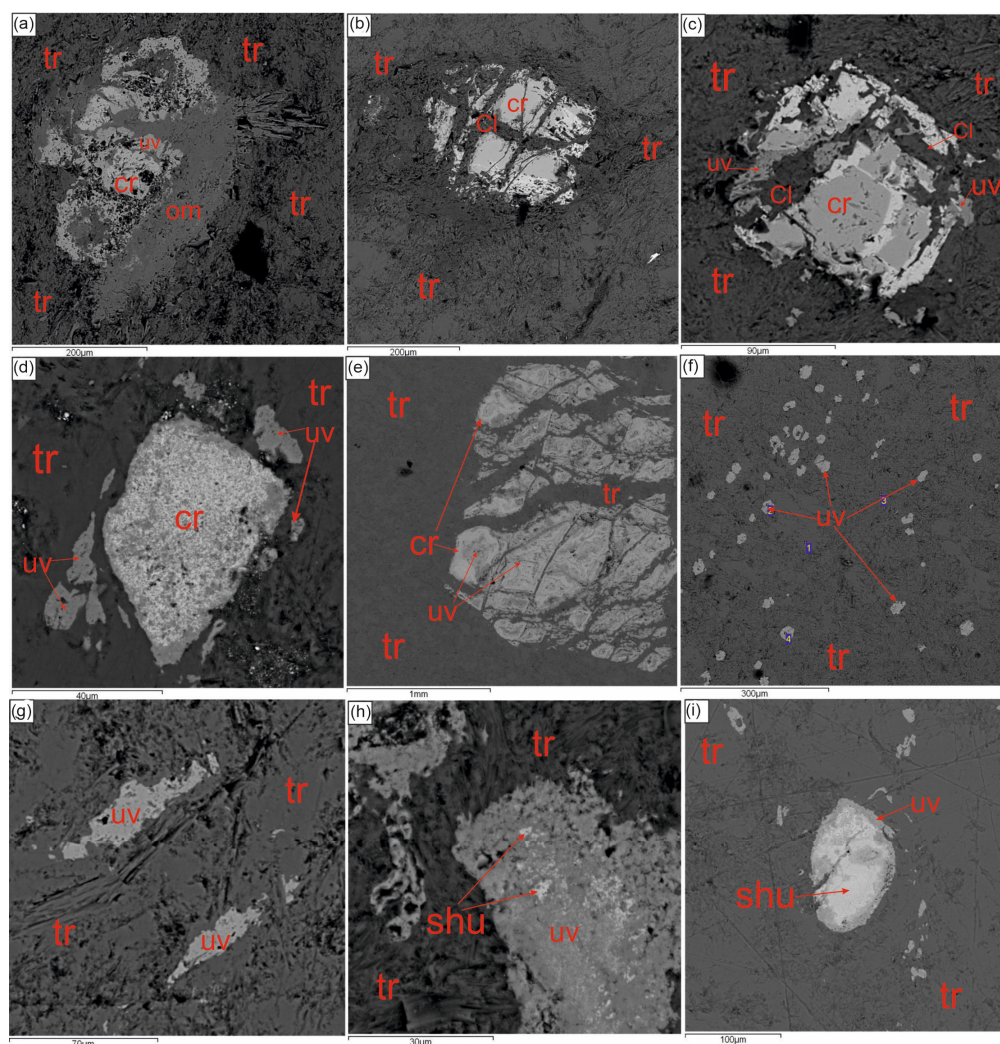


Figure 7. Mineral composition of nephrite: (a)—in tremolite, chromite is corroded by uvarovite, and overgrows omphacite, sample 557-1; (b)—chromite with chromium-ferruginous edges, stringers and chlorite overgrown in tremolite, sample 61-2; (c)—chromite with ferruginous chromite edges is replaced by uvarovite, overgrown with chlorite, with tremolite around it, sample 558; (d)—chromite spots are replaced by uvarovite, with individual grains of uvarovite among tremolite, sample 2-21; (e)—uvarovite-chromite grain, where chromite is on the periphery, with diopside grains in tremolite, sample 1-21; (f)—sheath-like crystals of uvarovite in tremolite, 510-1; (g)—elongated grains of uvarovite in tremolite, sample 557-1; (h)—chromite-“shuiskite”-uvarovite grain in tremolite, sample 1-21; (i)—“shuiskite”-uvarovite grain in tremolite, uvarovite on the periphery, sample 510-1. Cl—chlorite, cr—chromite, dp—diopside, om—omphacite, tr—tremolite, shu—unnamed mineral from shuiskite group, uv—uvarovite.

Chlorite ($\text{Mg}_{4.37}\text{Fe}^{2+}_{0.58}\text{Ca}_{0.04}\Sigma_{4.99}\text{Al}_{1.00}(\text{Si}_{3.37}\text{Al}_{0.22}\text{Cr}_{0.12})\Sigma_{3.71}\text{O}_{10}(\text{OH})_8$ (Table 4) composes separate cloud-shaped isometric-to-elongated sections, cuts and overgrows chromite (Figure 7b,c), and, less often, forms veinlets with grains of chromite and pentlandite. Chlorite, cutting or overgrowing chromite, contains more chromium and magnesium.

Chromite grains (Table 4) are rarely idiomorphic and homogeneous; they are more often fragmented, with an increased chromium and iron content (Figure 7b), or only iron, (Figure 7c) on the periphery; the chromite cracks with chlorite and overgrows the chromite. Chromite contains increased concentrations of manganese and zinc. Chromite is sometimes replaced by uvarovite along the periphery or in spots throughout the grain (Figure 7e).

Uvarovite forms mostly idiomorphic individual grains, sometimes sheath-like grains (Figure 7f), and replaces chromite. Xenomorphic elongated grains are less common (Figure 7g).

The uvarovite forming independent grains differs from the uvarovite which replaces the chromite because it contains more Ti and Fe, especially trivalent (sometimes up to an intermediate composition of uvarovite and andradite), Mg and V, less Al, Mn, and Cr.

Rare barite ($\text{Ba}_{1.00}\text{Sr}_{0.04}\text{S}_{0.99}\text{O}_4$) (BaO—62.58 wt. %, SrO—1.48 wt. %, SO_3 —34.32 wt. %), millerite ($\text{Ni}_{0.92}\text{Co}_{0.05}\text{S}_{1.03}$) (Co—3.50 wt. %, Ni—60.69 wt. %, S—37.13 wt. %), and an unnamed Fe-dominant mineral of the shuiskite group $\text{Ca}_{2.96}(\text{Fe}_{3.38}\text{Mn}_{0.23}\text{Al}_{0.20}\text{Zn}_{0.11}\text{Mg}_{0.04}\text{Ti}_{0.04})\text{Si}_{4.00}(\text{Cr}_{3.66}\text{Al}_{0.35})\text{Si}_{4.01}[\text{Si}_{1.03}\text{O}_4][\text{Si}_{2.00}\text{O}_6(\text{OH})](\text{OH})_3$ (Table 4, Figure 7h,i) [46] are associated with chromite-uvarovite grains. Pentlandite ($\text{Fe}_{3.42}\text{Co}_{0.30}\text{Ni}_{5.30}\text{S}_{9.02}\text{S}_{7.97}$) (based on eight analyses, Fe—22.19–24.78 wt. %, Co—2.29–3.22 wt. %, Ni—40.10–41.55 wt. %, and S—32.26–33.81 wt. %) forms xenomorphic, elongated, deformed and crushed grains.

3.5. Isotope Composition of the Rocks

We studied the oxygen isotope composition of the rocks of the Nyrdomenshor deposit (Table 5). The isotope composition of diopsidites is -6.8 and 7.8‰ $\delta^{18}\text{O}$. The hydrogarnet rodingite values were even lower -6.6‰ $\delta^{18}\text{O}$. The nephrites had a heavier isotope composition: 8.2 – 9.7‰ $\delta^{18}\text{O}$ (based on six analyses). The isotope composition of the jadeite was close to nephrite -8.8‰ $\delta^{18}\text{O}$.

Table 5. Isotopic composition of Nyrdomenshor deposit rocks.

No	Sample	Rock	$\delta^{18}\text{O}$, ‰ VSMOW
1	162	diopsidite	7.3
2	3/21	diopsidite	6.8
3		hydrogarnet rodingite	6.1
4	558	nephrite	8.9
5	2/21	nephrite	8.6
6	510-1	nephrite	8.4
7	1/21	nephrite	8.2
8	61-2	nephrite	8.5
9	557-1	nephrite	9.7
10	66	jadeite	8.8

4. Discussion

The nephrite of the Nyrdomenshor deposit is characterized by heterogeneous, unattractive coloration, jointing from foliation, and low translucency. Therefore, in terms of its quality characteristics, it does not correspond to standard jewelry or ornamental nephrite.

In Russia, the S-type nephrite is mainly mined in the Eastern Sayans, in the Oka district of the Republic of Buryatia. The nephrite of the Ospa deposit is of the best quality. The color is different shades of green, mostly bright bluish-green, brownish in some places, or with white veins and spots. The nephrite is massive, and less often is indistinctly striped cryptocrystalline. The structure is tangled and fibrous. Tremolite makes up 95%–100%, and there is a fine uniform inclusion of chrome spinel, replaced by magnetite (1%), up to 2 mm in size [20,47]. There is a “cat’s eye” effect [48].

The color of the nephrite of the Gorlykgol deposit is heterogeneous, spotted, and mostly green of different tones, although a black color also occurs. The nephrite is cryptocrystalline and massive, less often being shale. The structure is tangled and fibrous, and fibroblastic. It is transparent to a depth of 4–10 mm [47].

The color of the nephrite of the Bortogol deposit is green, of various tones. The contact areas have a shale texture, and prismatic tremolite and chlorite are present there [20]. There is a “cat’s eye” effect.

The nephrite of the Sagan-Sair deposit has a non-uniform color, from gray-green to dark green, with bluish-green spots and greenish veins. The texture ranges from massive to shale, and the structure is cryptocrystalline. The inclusions of ore minerals account for up to 2%, and it is transparent to a depth of 2–3 mm. The nephrite is of low quality, due to

fracturing, and shows a presence of large-crystalline lamellar tremolite, chlorite, talc, and serpentine. However, at the same time there are signs of the “cat’s eye” effect.

The nephrite of the Ulan-Khoda deposit is different. In the central part, it is massive, light green like a green apple, and with the marginal parts composed of shale nephrite of a brownish-green color. The structure is tangled and fibrous, i.e., nemato-fibroblastic. There are uniformly scattered rounded grains of chrome spinel, up to 1 mm in size. Light-green nephrite is transparent in plates with a thickness of more than 2 cm, and brown-green—to a depth of 1 cm. Light-green nephrite is replaced by a brownish-green nephrite also near the cracks and in the areas of catalase. The nephrite recrystallizes in the areas of maximum cataclysm, and becomes grayish without ore inclusions [20,49].

Nephrite is mined in the western Hamar-Daban, Zakamensky district of the Republic of Buryatia. The color of the nephrite of the Khamarkhuda deposit ranges from green to brownish-grayish with yellowish, greenish shades, as well as black. Bluish-green nephrite is characteristic and massive, with rare fine-ore mineral inclusions. The structure is tangled and fibrous, i.e., fibroblastic, and the texture is massive. In an amount of up to 1%, there is chlorite, chrome spinel, magnetite, clinocoisite, and sulfides. The marginal parts of the veins are composed of dark-green spotted nephrite with clinocoisite and magnetite. The black color is caused by the intensive development of fine graphite. The graphite is evenly distributed in the rock, often forming flakes, clusters at the grain boundary, and cracks. There is a “cat’s eye” effect [20].

The color of the nephrite of the Khargantinskoye deposit is uneven—trickled, spotted, and zonal; the core is blue-green, the 15–20 cm wide border is brownish-green and, grayish-green. The texture is massive and the structure is cryptocrystalline. It is transparent to a depth of 1–8 mm. There are inclusions of calcite, chlorite, ore minerals, and asbestos streaks [47].

Nephrite is occasionally mined in the Western Sayan, in the Krasnoyarsk region and Tuva. The color of the nephrite of the Kurtushiba deposit is bluish-green, grayish-green, and gray, with varying degrees of tone density. The nephrite is dense, massive cryptocrystalline. The structure is tangled and fibrous. Chlorite, magnetite and chrome spinel are observed there [20].

The color of the nephrite of the Kantegir deposit is heterogeneous: light green and bluish-green. The nephrite consists of tangled fibrous actinolite-tremolite (70%–75%), finely prismatic tremolite (5%–10%), with single grains of chrome spinel in the chlorite border, and magnetite (3%). The rock is transparent to a depth of 3–5 mm [20].

Previously, the Akademia deposit was developed in the Southern Urals, in the Chelyabinsk Oblast. The nephrite color is uniform, a mottled bluish-green, green, light green, rarely almost white, brownish-yellow and brownish-gray. There are veins of white, gray-hite, bluish-white to brownish-yellow and brown colors. The structure of the nephrite involves tangled fibrous, radially radiant leafy aggregates and larger felt-like clusters of the finest tremolite crystals. The nephrite is transparent up to 2 cm deep. Inclusions of ore minerals are characteristic: chromite, magnetite, nickeline, cobaltite, maucherite, pyrite and chalcopyrite. Sometimes there is up to 5% of actinolite and relics of antigorite in amounts up to 35%. Chromite is replaced by garnet of the uvarovite-grossular series. Vesuvianus is found in association with the garnet. Secondary minerals are scaly, flake-like tremolite, and zoisite [20,39].

Nephrite is extracted at the Bazhenovskoye deposit of chrysotile asbestos in the Middle Urals in the Sverdlovsk Oblast. The nephrite color is homogeneous-to-heterogeneous green, light green, bluish-green, grayish-green, and greenish. There are spots, veins, and lenses of a bright bluish-green or light-green color. The texture is massive, spotted and striped. The bulk (65%–75%, and less often more than 80%) of the nephrite is represented by tremolite. The mineral forms a fibroblastic tangled fibrous, sometimes porphyroblastic, sheaf-like structure. In the bulk, there is antigorite, sometimes forming finely scaled aggregates; in this case, its content can reach 25%–35%. There are diopside and talc. There is a rare, homogeneously distributed inclusion of black chromite, from 3 to 5%, with a grain size of

up to 2 mm, replaced by chromic grossular. Inclusions of thin, less than 1 mm, grains of nickeline and maucherite are evenly spaced. The nephrite is transparent to a depth of 0.5 to 2 cm [35].

The mineral composition of the Nyrdvomenshor nephrite is peculiar. Minerals such as omphacite, barite, and millerite have not been previously observed in S-type nephrite. Fe-dominant mineral from the shuiskite group has not been described at all before.

Uvarovite is of even greater interest. It forms visually distinguishable secretions, and is present in all samples in large quantities, forming independent grains and replacing the chromite. Uvarovite was previously described in the nephrite of the Fentien deposit, Taiwan [12]. However, the published garnet analysis results correspond to chromium grossular (11.6 wt. % Cr₂O₃ on average; the maximum content is 12.86 wt. %, and the higher crystal core analysis results correspond to a mixture of chromium grossular and chromite). Uvarovite was mentioned as a mineral of the nephrite of the Nyrdvomenshor and the deposits of British Columbia, Canada [20] and Ya'an, Sichuan Province, China [50] without any analysis data attached.

Garnet of a grossular-uvarovite composition was found in the nephrite of the Nasławice deposit in Poland [28], the Bazhenov chrysotile-asbestos deposit [35] and the Pounamu Ultramafics, Westland, New Zealand [30]. So far, the only reliable finding of abundant low-alumina uvarovite in S-type nephrite has been recorded at the Manas deposit in the Northern Tien Shan in the north of the Xinjiang Uygur Autonomous Region of China [7]. A single uvarovite analysis is also reported from the nearby Puserka jadeite deposit, related to the Syum-Key ultramafic massif [51].

The S-type of nephrite was specified according to its chemical composition. It is believed that S-type nephrite has usual values of $Fe^{2+}/(Mg + Fe^{2+}) > 0.06$, whereas for the D-type nephrite it is < 0.06 [52]. The Nyrdvomenshor nephrite value of $Fe_2O_3\Sigma/(MgO + Fe_2O_3\Sigma)$ varies within the range of 0.19–0.21 (Table 3).

The content of Cr, Ni, and Co in nephrite can also be used to distinguish S-type and D-type nephrite [52]. The Cr (900–2812 ppm), Ni (958.7–1898 ppm) and Co (42–207 ppm) contents in the S-type nephrite are relatively high, while the Cr (2–179 ppm), Ni (0.05–471 ppm) and Co (0.5–10 ppm) contents in the D-type nephrite are relatively low [52–55].

The content range is wider for the Russian deposits. For the S-type nephrite on average: Ospa deposit—1170 ppm of Cr, 1020 ppm of Ni, 65 ppm of Co (16 samples); Gorlykgol—270 ppm, 1050 ppm, 97 ppm (3); Bortogol—580 ppm, 100 ppm, 53 ppm (3); Ulankhoda—1200 ppm, 1400 ppm, 62 ppm (26); Kitoy—30 ppm, 120 ppm, 5 ppm (1); Khamarkhuda—660 ppm, 590 ppm, 54 ppm (32); Param—1500 ppm, 1250 ppm, 64 ppm (8); Kelyana—1700 ppm, 1800 ppm, 56 ppm (1); Kurtushiba—970 ppm, 1230 ppm, 61 ppm (3); Agardak—1100 ppm, 420 ppm, 42 ppm (1); Khalilov—180 ppm, 600 ppm, 22 ppm (10); and Kozmodemyanov—800 ppm, 900 ppm, 50 ppm (1). For the D-type nephrite of Russian deposits, on average: 32 ppm, 19 ppm, and 6 ppm [20].

The content of these elements in the Nyrdvomenshor nephrite (based on our data) is reduced (Cr 400–700 ppm, Ni 400 ppm, Co 21–24 ppm, Table 3), due to the interaction of the serpentinite melange with terrigenous and intrusive rocks, but it still corresponds to the S-type nephrite. Previously, higher values were shown: 1110, 570, and 68, based on 7 analyses [20]. Thus, the Nyrdvomenshor nephrite is typically the S-type.

The content of rare earth elements (REE) ranges from 0.460 to 0.948 ppm (Table 3), and the distribution pattern is flat with a weak right slope—this is from the enrichment with light REE, a positive Eu anomaly (Figure 8).

A positive Eu anomaly is observed at the Manas deposit, and a negative one at the Eastern Sayan deposits, with a right slope [7]. A positive Eu anomaly indicates a complex source of ore-forming fluid [7]. The Kutcho deposit has a left slope—this indicated enrichment with heavy REE, which is explained by the acidic environment of nephrite formation; the weakly negative Eu anomaly is attributed to the reducing metallogenic environment [24]. The REE profiles of the Kutcho and Polar (Canada), Rim and South Westland (New Zealand), Golmud (Qinghai, China), Manas (Xinjiang, China) and Ulankhoda

(Eastern Sayan, Russia) deposits were compared [24]. The Σ REE contents ranged from 0.250 to 7.660 ppm—the Kutcho nephrite had a higher Σ REE value (2.141–2.920 ppm), while the Σ REE value of New Zealand nephrite was the lowest (0.378–0.671 ppm). Since the value of Σ REE increases with decreasing pH, it is assumed that the metallogenic environment of the Kutcho nephrite was very acidic. In relatively restorative conditions, δ Eu shows a negative anomaly, which is shown for all five deposits. Golmud, Manas and Ulankhoda show a right slope [24]. Based on the peculiarities of the distribution of REE in the Nyrdvomenshor nephrite, it can be assumed that it was formed under the influence of a complex, non-acidic solution in an oxidizing environment.

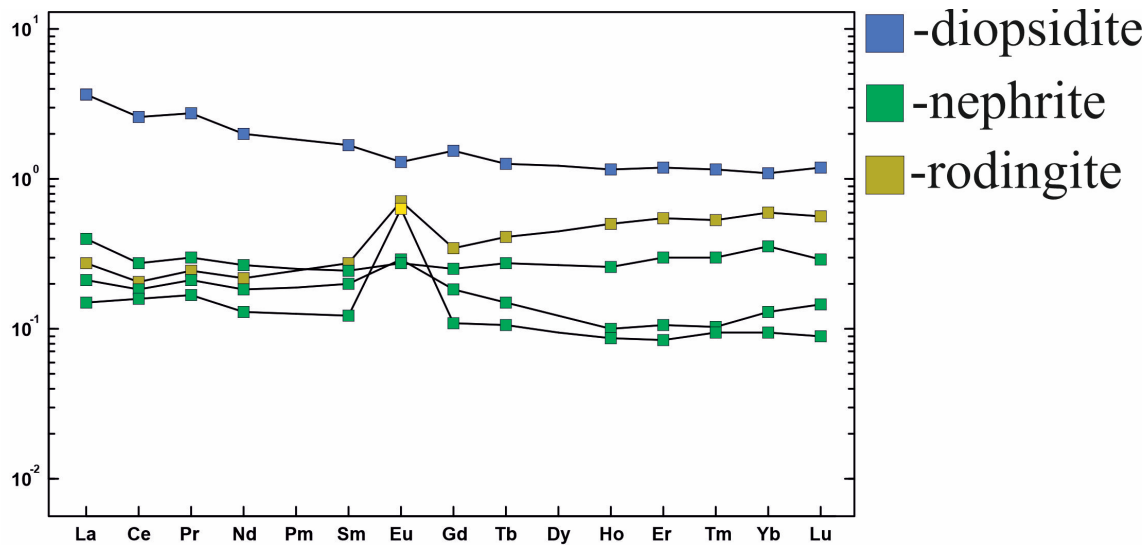
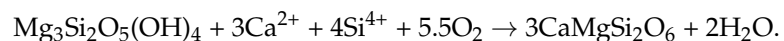


Figure 8. Normalized distribution of rare earth elements.

The mineral composition reveals a complicated formation history of the nephrite involving the combination of tectonic and metasomatic processes. At the progressive stage, serpentine is replaced by diopside:



Fluids containing calcium and silica come either from late intrusive bodies or as a result of long-range transport along tectonic ruptures.

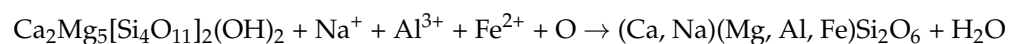
At the regressive or metamorphic stage, the diopside is replaced by a tremolite aggregate—nephrite:



This is indicated by the relic grains of diopside. The official IMA formula of tremolite is $\text{Ca}_2(\text{Mg}_{5.0-4.5}\text{Fe}^{2+}_{0.0-0.5})\text{Si}_8\text{O}_{22}(\text{OH})_2$, but in the equation we use the formula of the tremolite with no end-member, so as not to introduce the Fe.

The relic chromite is crushed with an increase in the content of the manganese and zinc, and replaced by uvarovite and an unnamed mineral from the shuiskite group. Heazlewudite is replaced by pentladite—tremolite and pentlandite appear in a small amount in one sample of diopside. Chlorite and part of the uvarovite of the nephrite are inherited from the diopside.

The third progressive stage led to the replacement of the tremolite with omphacite (the reaction is not balanced, due to the variable composition of the omphacite)



and to the crushing of the nephrite, which worsened its quality as an ornamental stone.

A further process in the development, with an increase in the sodium and aluminum content, should lead to the formation of jadeite $\text{NaAlSi}_2\text{O}_6$. Previously, the Nyrdomenshor jadeite was believed [36] to have been formed before the nephrite.

The joint occurrence of jadeite and nephrite boulders in the region, noted in the Nyrdomenshor deposit, has long been known [56]. But even at the Nyrdomenshor deposit, their bedrock outcrops are separated spatially: nephrite outcrops are located to the east, and jadeite outcrops to the west, where the pressure was higher. Syum-Keu jadeites were previously studied: their origin under the influence of subduction fluids was shown either in association with omphacite from subduction peridotites [57], or after trondhjemite, with omphacite as an intermediate phase [58].

At the Nyrdomenshor deposit, the isotope composition of the diopsidites—6.8 and 7.3‰ $\delta^{18}\text{O}$, and of the hydrogarnet rodingite—6.6‰ $\delta^{18}\text{O}$ indicates the deep origin of the oxygen inherited from the ultramafites that underwent serpentinization and metasomatism—diopsidization with a small addition of the crustal component. The nephrites, apparently formed as a result of the further metasomatism of the diopsidites, have a heavier isotope composition—8.2–9.7‰ $\delta^{18}\text{O}$. This indicates that the crustal fluid contribution to the metasomatism is increasing. The isotope composition of the jadeite is close to that of the nephrite—8.8‰ $\delta^{18}\text{O}$, since when nephrite is replaced with jadeite, it does not indicate absorption, but disposal of the fluid.

An important indicator of the nephrite formation processes is the isotopic composition of oxygen. At the Fengtien deposit in Taiwan, for the ordinary nephrite the $\delta^{18}\text{O}$ is 4.5%–5.3%, for the wax-like nephrite it is 4.7%–5.0%, and for the nephrite with the “cat’s eye” effect it is 5.1%–5.3%. For the diopside from diopsidite it is 3.7%–4.5%. It is concluded that nephrite inherits its composition from serpentinites and diopsidites [13]. The oxygen isotopic composition has been identified for a number of deposits of S-type nephrite in Russia: Param in Northern Transbaikalia, $\delta^{18}\text{O}$ —6.13%–9.54‰; Ospa in the Eastern Sayans—8.43; and Khamarkhudia in the Khamar-Daban—6.72–7.87. It is believed that the fluid phase of the nephrites indicates their transformation from serpentinites during metamorphism [59]. At the Jordanov deposit in Poland the $\delta^{18}\text{O}$ is 6.1‰, and for the shale nephrite it is 6.7 [26]. The isotopic composition of oxygen for the S-type nephrite in the Chinese province of Qinghai is ($\delta^{18}\text{O}$) 8.1, 8.6‰; in Russia it is 8.2–8.5; in Canada it is 9.4–12.3; in New Zealand it is 4.7, 8.0; in Australia it is 1.3, 1.6; and in Pakistan it is 13.0–13.4. It is shown that ore-forming fluids are formed as a result of metamorphism [60]. Single analyses were performed for the S-type nephrite from the Chara Dzhelgra River (false name?) in Siberia ($\delta^{18}\text{O}$ —6.9), Red Mountain in New Zealand (7.5), Mount Ogden, Canada (9.6), and the Shulaps Range, Canada (8.4). These values are explained by the inheritance of the isotopic composition of the initial serpentinite with the possible influence of the contact with the metagabbro or crystalline shales [61].

Metamorphism reinforced the metasomatic processes in the serpentinite melange, with the formation of a cryptocrystalline tangled-fibrous structure of the nephrite, but then led to its fragmentation and replacement with omphacite. There are eight stages of the deformation process for the region [62], during which the regressive and progressive regimes were able to replace each other.

The results obtained allow the subsurface user to refuse the license or adjust the territory of the subsurface site, and allow the authorities of the Yamal-Nenets Autonomous Okrug to expand the natural park and make it more attractive, due to additional knowledge.

5. Conclusions

The green nephrite of the Nyrdomenshor deposit is tremolite in composition. The accessory minerals are diopside, chromite, uvarovite, omphacite, pentlandite, barite, millerite, the unnamed Fe-dominant mineral of the shuiskite group, chlorite. The nephrite isotope composition is 8.2–9.7‰ $\delta^{18}\text{O}$. It is linked to the serpentinite type. The Nyrdomenshor nephrite value $\text{Fe}_2\text{O}_3\Sigma / (\text{MgO} + \text{Fe}_2\text{O}_3\Sigma)$ varies within the range of 0.19–0.21, and the content of Cr is 400–700 ppm, Ni is 400 ppm, and Co is 21–24 ppm. The content of

rare earth elements ranges from 0.460 to 0.948 ppm, and the distribution pattern is flat, with a weak right slope—due to enrichment with light REE, a positive Eu anomaly. The green nephrite of the Nyrdvomenshor deposit was formed by both multistage metasomatic and superimposed metamorphic processes. Initially, diopside formed after serpentinite, and then it was replaced by the nephrite. Metamorphism reinforced the metasomatism in the serpentinite melange and provided the cryptocrystalline tangled-fibrous structure of the nephrite. Then, metamorphism and metasomatism resulted in omphacite formation and nephrite cracking, which reduced its quality. As these processes progressed, the contribution of the crustal fluid increased.

Author Contributions: Conceptualization, E.V.K., M.P.P. and F.M.N.; methodology, E.V.K.; software, V.V.V.; validation, E.V.K.; formal analysis, E.V.K.; investigation, E.V.K., M.P.P. and V.F.P.; resources, M.P.P. and F.M.N.; data curation, E.V.K. and M.P.P.; writing—original draft preparation, E.V.K.; writing—review and editing, E.V.K.; visualization, V.V.V.; supervision, E.V.K.; project administration, E.V.K.; funding acquisition, E.V.K. All authors have read and agreed to the published version of the manuscript.

Funding: This research was funded by the Russian Science Foundation, grant number 22-27-20003, <https://rscf.ru/project/22-27-20003>, accessed on 1 June 2022.

Data Availability Statement: The data supporting reported results can be provided by the corresponding author upon request.

Acknowledgments: The authors are grateful for the help with the work from the technicians D.M. Vurms and A.V. Trofimov, and the analysts N.P. Gorbunova, L.A. Tatarinova, I.A. Zhelunitsyn, A.A. Nekrasova, D.V. Kiseleva and E.A. Khromova. Comments and suggestions of three reviewers contributed to a significant improvement in the manuscript. The authors are grateful to the Federal State Budgetary Educational Institution of Higher Education, the “Ural State Mining University” for creating the conditions for performing the work as part of the federal program of strategic academic leadership “Priority 2030”. The equipment of the Central Collective Use Centers “Geoanalyst” of the IGG UrB RAS, Yekaterinburg, and “Geospektr” of the GIN SB RAS, Ulan-Ude, was used.

Conflicts of Interest: The authors declare no conflict of interest.

References

1. Kievlenko, E.Y. *Geology of Gems*; Ocean Pictures Ltd.: Littleton, CO, USA, 2003; 468p.
2. Harlow, G.E.; Sorensen, S.S. Jade (Nephrite and Jadeitite) and Serpentinite: Metasomatic Connections. *Int. Geol. Rev.* **2005**, *47*, 113–146. [[CrossRef](#)]
3. Zhong, Q.; Liao, Z.; Qi, L.; Zhou, Z. Black nephrite jade from Guangxi, Southern China. *Gems Gemol.* **2019**, *55*, 198–215. [[CrossRef](#)]
4. Flint, D.J.; Dubowski, E.A. *Cowell Jade Province: Detailed Geological Mapping and Diamond Drilling of Jade and Ornamental Marble Outcrops, 1982–1987; Report Book, 89/51*; Department of Mines and Energy of South Australia: Adelaide, Australia, 1991.
5. Zhang, Y.-D.; Yang, R.-D.; Gao, J.-B.; Chen, J.; Liu, Y.-N.; Zhou, Z.-R. Geochemical characteristics of nephrite from Luodian County, Guizhou Province, China. *Acta Miner. Sin.* **2015**, *35*, 56–64, (In Chinese with English abstract).
6. Tan, T.L.; Ng, L.L.; Lim, L.C. Studies on Nephrite and Jadeite Jades by Fourier Transform Infrared (FTIR) and Raman Spectroscopic Techniques. *Cosmos* **2013**, *9*, 47–56. [[CrossRef](#)]
7. Wang, J.; Shi, G. Comparative Study on the Origin and Characteristics of Chinese (Manas) and Russian (East Sayan) Green Nephrites. *Minerals* **2021**, *11*, 1434. [[CrossRef](#)]
8. Yu, H.; Wang, R.; Guo, J.; Li, J.; Yang, X. Study of the minerogenetic mechanism and origin of Qinghai nephrite from Golmud, Qinghai, Northwest China. *Sci. China Earth Sci.* **2016**, *59*, 1597–1609. [[CrossRef](#)]
9. Zhang, C.; Yu, X.; Yang, F.; Santosh, M.; Huo, D. Petrology and geochronology of the Yushigou nephrite jade from the North Qilian Orogen, NWChina: Implications for subduction-related processes. *Lithos* **2021**, *380–381*, 105894. [[CrossRef](#)]
10. Xu, Y.X.; Lu, B.Q.; Qi, L.J. A petromineralogical and SEM microstructural analysis of nephrite in Sichuan Province. *Shanghai Land Resour.* **2015**, *36*, 87–89, (In Chinese with English Abstract).
11. Zhang, C.; Yang, F.; Yu, X.; Liu, J.; Carranza, E.J.M.; Chi, J.; Zhang, P. Spatial-temporal distribution, metallogenic mechanisms and genetic types of nephrite jade deposits in China. *Front. Earth Sci.* **2023**, *11*, 1047707. [[CrossRef](#)]
12. Wan, H.M.; Yeh, C.L. Uvarovite and grossular from the Fengtien nephrite deposits, Eastern Taiwan. *Mineral. Mag.* **1984**, *48*, 31–37. [[CrossRef](#)]
13. Yui, T.-F.; Yeh, H.-W.; Lee, C.W. Stable isotope studies of nephrite deposits from Fengtien, Taiwan. *Geochim. Cosmochim. Acta* **1988**, *52*, 593–602. [[CrossRef](#)]

14. Yui, T.F.; Usuki, T.; Chen, C.Y.; Ishida, A.; Sano, Y.; Suga, K.; Iizuka, Y.; Chen, C.T. Dating thin zircon rims by NanoSIMS: The Fengtien nephrite (Taiwan) is the youngest jade on earth. *Int. Geol. Rev.* **2014**, *56*, 1932–1944. [[CrossRef](#)]
15. Umar, Z.A.; Liaqat, U.; Ahmed, R.; Baig, M.A. Classification of Nephrite Using Calibration-Free Laser Induced Breakdown Spectroscopy (CF-LIBS) with Comparison to Laser Ablation–Time-of-Flight–Mass Spectrometry (LA–TOF–MS). *Anal. Lett.* **2019**, *53*, 203–216. [[CrossRef](#)]
16. Obiadi, S.S.; Amini, M.A.; Fazli, F. Mineralogy and Geochemistry of Nephrite from Wolay Deposit, Kunar, East Afghanistan. *J. Mech. Civ. Ind. Eng.* **2022**, *3*, 56–65.
17. Rehman, H.U.; Bilal; Owais, O.; Rahman, O.U.; Shen, A.H. Namak Mandi: A pioneering gemstone market in Pakistan. *Gems Gemol.* **2021**, *57*, 138–149. [[CrossRef](#)]
18. Khan, R.A.; Anwar-Ul-Haq, M.; Qasim, M.; Afgan, M.S.; Haq, S.U.; Hussain, S.Z. Spectroscopic and crystallographic analysis of nephrite jade gemstone using laser induced breakdown spectroscopy, Raman spectroscopy, and X-ray diffraction. *Heliyon* **2022**, *8*, e11493. [[CrossRef](#)]
19. Kovalenko, I.V.; Khadzhi, I.P.; Kovalenko, V.S.; Sviridenko, A.F. Features of the microstructure and composition of ultramafic related nephrite. *Zap. All-Union. Mineral. Soc.* **1985**, *114*, 707–712. (In Russian)
20. Suturin, A.N.; Zamaletdinov, R.S.; Sekerina, N.V. *Nephrite Deposits*; ISU Press: Irkutsk, Russia, 2015; 377p. (In Russian)
21. Pham, V.L.; Giuliani, G.; Garnier, V.; Ohnenstetter, D. Gemstones in Vietnam—A review. *Austral. Gemmol.* **2004**, *22*, 162–168.
22. Boyd, W.F.; Wight, W. Gemstones of Canada. *J. Gemmol.* **1983**, *18*, 544–562. [[CrossRef](#)]
23. Simandl, G.J.; Riveros, C.P.; Schiarizza, P. *Nephrite (Jade) Deposits, Mount Ogden Area, Central British Columbia (NTS 093N 13W)*; Geological Fieldwork 1999, Paper 2000-1; British Columbia Geological Survey: Victoria, BC, Canada, 2000; pp. 339–347.
24. Jiang, B.; Bai, F.; Zhao, J. Mineralogical and geochemical characteristics of green nephrite from Kutcho, northern British Columbia, Canada. *Lithos* **2021**, *388–389*, 106030. [[CrossRef](#)]
25. Mills, J. A Unique Occurrence of Nephrite Jade with Magnetite Inclusions in San Bernardino County, California. *Rocks Miner.* **2021**, *96*, 442–449. [[CrossRef](#)]
26. Gil, G.; Barnes, J.D.; Boschi, C.; Gunia, P.; Szakmany, G.; Bendo, Z.; Raczynski, P.; Peterdi, B. Origin of serpentinite-related nephrite from Jordanów and adjacent areas (SW Poland) and its comparison with selected nephrite occurrences. *Geol. Q.* **2015**, *59*, 457–472. [[CrossRef](#)]
27. Lobos, K.; Sachanbinski, M.; Pawlik, T. Nephrite from Naslawice in Lower Silesia (SW Poland). *Prz. Geol.* **2008**, *56*, 991–999, (In Polish with English abstract).
28. Gil, G.; Baginski, B.; Gunia, P.; Madej, S.; Sachanbinski, M.; Jokubauskas, P.; Belka, Z. Comparative Fe and Sr isotope study of nephrite deposits hosted in dolomitic marbles and serpentinites from the Sudetes, SW Poland: Implications for Fe–As–Au-bearing skarn formation and post-obduction evolution of the oceanic lithosphere. *Ore Geol. Rev.* **2020**, *118*, 103335. [[CrossRef](#)]
29. Adams, C.J.; Beck, R.J.; Campbell, H.J. Characterisation and origin of New Zealand nephrite jade using its strontium isotopic signature. *Lithos* **2007**, *97*, 307–322. [[CrossRef](#)]
30. Cooper, A.F. Origin and evolution of nephrites, diopsidites and giant diopside crystals from the contact zones of the Pounamu Ultramafics, Westland, New Zealand. *N. Z. J. Geol. Geophys.* **2023**, *66*, 88–101. [[CrossRef](#)]
31. Tarling, M.S.; Smith, S.A.F.; Negrini, M.; Kuo, L.-W.; Wu, W.-H.; Cooper, A.F. An evolutionary model and classification scheme for nephrite jade based on veining, fabric development, and the role of dissolution–precipitation. *Sci. Rep.* **2022**, *12*, 7823. [[CrossRef](#)]
32. Hockley, J.J. Nephrite (jade) Occurrence in the Great Serpentine Belt of New South Wales, Australia. *Nature* **1974**, *247*, 364. [[CrossRef](#)]
33. Coenraads, R.R. Gemstones of New South Wales. *Austral. Gemmol.* **1995**, *19*, 91–107.
34. Makagonov, E.P.; Arkhireev, I.E. Nephrite of the Urals. In *Geoarchaeology and Archaeological Mineralogy*; Springer: Berlin/Heidelberg, Germany, 2014; Volume 1, pp. 15–19. (In Russian)
35. Kislov, E.V.; Erokhin, Y.V.; Popov, M.P.; Nikolayev, A.G. Nephrite of Bazhenovskoye Chrysotile–Asbestos Deposit, Middle Urals: Localization, Mineral Composition, and Color. *Minerals* **2021**, *11*, 1227. [[CrossRef](#)]
36. Kazak, A.P.; Dobretsov, N.L.; Moldavantsev, Y.E. Glaucofane shists, jadeites, vesuvianites and nephrites of the Rai-Iz hyperbasite massif. *Geol. Geophys.* **1976**, *2*, 60–66. (In Russian)
37. Yushkin, N.P.; Ivanov, O.K.; Popov, V.A. *Introduction to Topomineralogy of the Urals*; Nauka: Moscow, Russia, 1986; 295p. (In Russian)
38. Knyazev, Y.G.; Knyazeva, O.Y.; Snachev, V.I.; Zhdanov, A.V.; Karimov, T.R.; Aidarov, E.M.; Masagutov, R.K.; Arslanova, E.R. *State Geological Map of the Russian Federation. Scale 1:1 000 000 (Third Generation). Ural Series. Sheet N-40–Ufa. Explanatory Note*; VSEGEI Map Factory: Sankt-Petersbourg, Russia, 2013; 512p. (In Russian)
39. Arkhireev, I.E.; Maslennikov, V.V.; Makagonov, E.P.; Kabanova, L.Y. South Ural nephrite province. *Razved. I Okhrana Nedr* **2011**, *3*, 18–22. (In Russian)
40. Dobretsov, N.L.; Tatarinov, A.V. *Jadeite and Nephrite in Ophiolites (the Example of West Sayan)*; Nauka: Novosibirsk, Russia, 1983; 126p. (In Russian)
41. Kislov, E.V.; Popov, M.P.; Nurmukhametov, F.M.; Posokhov, V.F. Nephrite from the Nyrdvomenshor deposit (Polar Urals): Features of composition and formation settings. In Proceedings of the Ultramafic-Mafic Complexes: Geology, Composition, Ore Potential. Materials of Conference, Apatity, Russia, 29 August–3 September 2022; pp. 54–57. (In Russian)

42. Gorbunova, N.P.; Tatarinova, L.A.; Kudyakova, V.S.; Popov, M.P. Wave X-ray fluorescence spectrometer XRF-1800 (SHIMADZU, Japan): Method of determination of trace impurities in rubies. In *Yearbook-2014. Proceedings of IGG UrB RAS*; IGG UrB RAS: Yekaterinburg, Russia, 2015; Volume 162, pp. 238–241. (In Russian)
43. Sharp, Z.D. A laser-based microanalytical method for the in situ determination of oxygen isotope ratios of silicates and oxides. *Geochim. Cosmochim. Acta* **1990**, *54*, 1353–1357. [[CrossRef](#)]
44. Vakhrusheva, N.V.; Shiryaev, P.B.; Stepanov, A.E.; Bogdanova, A.R. *Petrology and Chromite Content of the Rai-Iz Ultrabasic Massif (Polar Urals)*; IGG UrB RAS: Ekaterinburg, Russia, 2017; 265p. (In Russian)
45. Sychev, S.N.; Kulikova, K.V. *The Sequence of Deformations in the Frame of the Rai-Iz Massif (Polar Urals)*; Series 7; Vestnik of Saint Petersburg University: St Petersburg, Russia, 2012; Volume 3, pp. 53–59. (In Russian)
46. Lykova, I.; Varlamov, D.; Chukanov, N.; Pekov, I.; Belakovskiy, D.; Ivanov, O.; Zubkova, N.; Britvin, S. Chromium Members of the Pumpellyite Group: Shuiskite-(Cr), $\text{Ca}_2\text{CrCr}_2[\text{SiO}_4][\text{Si}_2\text{O}_6(\text{OH})](\text{OH})_2\text{O}$, a New Mineral, and Shuiskite-(Mg), a New Species Name for Shuiskite. *Minerals* **2020**, *10*, 390. [[CrossRef](#)]
47. Yurgenson, G.A. *Jewelry and Ornamental Stones of Transbaikalia*; Nauka: Novosibirsk, Russia, 2001; 390p. (In Russian)
48. He, W.; Bai, F.; Zhao, C.; Qu, H.; Li, X. Petrogenesis of Chatoyant Green Nephrite from Serpentine-Related Deposits, Ospinsk, Russia: Insights from Mineralogy and Geochemistry. *Crystals* **2023**, *13*, 252. [[CrossRef](#)]
49. Khudyakova, L.I.; Kislov, E.V.; Paleev, P.L.; Kotova, I.Y. Nephrite-bearing mining waste as a promising mineral additive in the production of new cement types. *Minerals* **2020**, *10*, 394. [[CrossRef](#)]
50. Jin, X.; Qiu, Z.; Dai, S.; Yi, J.; Li, L.; Zhang, Y. Gemmological and mineralogical characteristics of nephrite from Ya'an, Sichuan Province. *J. Gems Gemmol.* **2014**, *16*, 20–27. (In Chinese with English abstract).
51. Popov, M.P.; Fomina, M.A.; Veretennikova, T.Y. Garnet mineralization from the Pusierka jadeite deposit (YaNAO). In *Ural Mineralogical School-2015: Collection of Articles by Students, Graduate Students and Scientists*; IGG UrB RAS: Ekaterinburg, Russia, 2015; pp. 200–202. (In Russian)
52. Siqin, B.; Qian, R.; Zhou, S.J.; Gan, F.X.; Dong, M.; Hua, Y.F. Glow discharge mass spectrometry studies on nephrite minerals formed by different metallogenic mechanisms and geological environments. *Int. J. Mass Spectrom.* **2012**, *309*, 206–211. [[CrossRef](#)]
53. Grapes, R.H.; Yun, S.T. Geochemistry of a New Zealand nephrite weathering rind. *N. Z. J. Geol. Geophys.* **2010**, *53*, 413–426. [[CrossRef](#)]
54. Liu, Y.; Deng, J.; Shi, G.; Yui, T.-F.; Zhang, G.; Maituohuti, A.; Yang, L.; Sun, X. Geochemistry and petrology of nephrite from Alamas, Xinjiang, NW China. *J. Asian Earth Sci.* **2011**, *42*, 440–451. [[CrossRef](#)]
55. Kostov, R.I.; Prochostov, C.; Stoyanov, C.; Csedreki, L.; Simon, A.; Szikszai, Z.; Uzonyi, I.; Gaydarska, B.; Chapman, J. Micro-PIXE geochemical fingerprinting of nephrite neolithic artifacts from Southwest Bulgaria. *Geoarchaeology* **2012**, *27*, 457–469. [[CrossRef](#)]
56. Dergunov, A.B.; Kazak, A.I.; Moldavantsev, Y.E. Serpentine melange and structural position of the Rai-Iz ultramafic massif (Polar Urals). *Geotectonics* **1975**, *1*, 28–34. (In Russian)
57. Meng, F.; Yang, H.J.; Makeyev, A.B.; Ren, Y.; Kulikova, K.V.; Bryanchaninova, N.I. Jadeitite in the Syum-Keu ultramafic complex from Polar Urals, Russia: Insights into fluid activity in subduction zones. *Eur. J. Miner.* **2016**, *28*, 1079–1097. [[CrossRef](#)]
58. Angiboust, S.; Glodny, J.; Cambeses, A.; Raimondo, T.; Monie, P.; Popov, M.; Garcia-Casco, A. Drainage of subduction interface fluids into the forearc mantle evidenced by a pristine jadeitite network (Polar Urals). *J. Metamorph. Geol.* **2021**, *39*, 473–500. [[CrossRef](#)]
59. Burtseva, M.V.; Ripp, G.S.; Posokhov, V.F.; Murzintseva, A.E. Nephrites of East Siberia: Geochemical features and problems of genesis. *Russ. Geol. Geophys.* **2015**, *56*, 402–410. [[CrossRef](#)]
60. Liu, X.-F.; Zhang, H.-Q.; Liu, Y.; Zhang, J.; Li, Z.-J.; Zhang, J.-H.; Zheng, F. Mineralogical characteristics and genesis of green nephrite from the world. *Rocks Miner. Anal.* **2018**, *37*, 479–489. (In Chinese with English abstract). [[CrossRef](#)]
61. Yui, T.-F.; Kwon, S.-T. Origin of a Dolomite-Related Jade Deposit at Chuncheon, Korea. *Econ. Geol.* **2002**, *97*, 593–601. [[CrossRef](#)]
62. Sychev, S.N. Structure and Evolution of the Main Ural Fault Zone (Southern Part of the Polar Urals). Abstract of Ph.D. Thesis, Geological Institute of Russian Science Academy, Moscow, Russia, 2015; 24p. (In Russian)

Disclaimer/Publisher's Note: The statements, opinions and data contained in all publications are solely those of the individual author(s) and contributor(s) and not of MDPI and/or the editor(s). MDPI and/or the editor(s) disclaim responsibility for any injury to people or property resulting from any ideas, methods, instructions or products referred to in the content.